

# Optimization of Nitrate Removal by Electro-Reduction Using a Ti/RuO<sub>2</sub> + IrO<sub>2</sub> Electrode: Process Modeling by Response Surface Methodology

Mar Bassine Boye, Abdou Khadre Djily Dimé\*, Galass Diouf, Ndeye Ngoné Diome, Mamadou Moustapha Sarr

Département de Chimie, UFR SATIC, Equipe Matériaux, Electrochimie et Photochimie Analytiques (EMEPA) de l'Université Alioune Diop de Bambey, Bambey, Sénégal  
Email: \*abdou.dime@uadb.edu.sn

**How to cite this paper:** Boye, M.B., Dimé, A.K.D., Diouf, G., Diome, N.N. and Sarr, M.M. (2026) Optimization of Nitrate Removal by Electro-Reduction Using a Ti/RuO<sub>2</sub> + IrO<sub>2</sub> Electrode: Process Modeling by Response Surface Methodology. *Journal of Materials Science and Chemical Engineering*, 14, 13-25.

<https://doi.org/10.4236/msce.2026.145002>

**Received:** March 30, 2026

**Accepted:** May 24, 2026

**Published:** May 27, 2026

Copyright © 2026 by author(s) and Scientific Research Publishing Inc. This work is licensed under the Creative Commons Attribution International License (CC BY 4.0).

<http://creativecommons.org/licenses/by/4.0/>



Open Access

## Abstract

Agricultural activities and the excessive use of fertilizers significantly contribute to nitrate contamination in the environment. These ions can cause a serious threat to both human health and ecosystems through the contamination of surface water and groundwater. It is therefore necessary to reduce their concentration before consumption. The general objective of this work is to propose new electrochemical treatment methods based on the Design of Experiments Methodology. Indeed, this approach allows to reduce the need for costly and lengthy experimental trials. Various parameters that could improve the efficiency of the process were studied, including initial concentration, pH, electrolysis time, and current intensity, in order to determine the optimal operating conditions. The results show that the process is effective at a reduction current intensity of  $-603$  mA, a NaNO<sub>3</sub> concentration of 100 mg-N/L, and an electrolysis time of 10 min at a slightly basic pH, allowing a nitrate removal efficiency of 91%. The results highlight the importance of statistical modeling in improving and controlling electrochemical processes.

## Keywords

Electrochemical Reduction, Water Treatment, Nitrate, Optimization, Modelling

## 1. Introduction

Water is a fundamental and essential resource for all living things life [1]. How-

ever, the extensive use of fertilizers in agricultural development can lead to the pollution of water resources by chemicals products through their infiltrating into water table [2] [3]. Groundwater contamination by nitrate ions, resulting from intensive agricultural practices, can compromise drinking water quality [4]. Nitrate becomes particularly toxic when reduced to nitrite; which can react with hemoglobin in the blood to form methemoglobin, thereby constituting a serious health risk, especially for children [5]. In Senegal, several studies carried out in agricultural regions have reported excessive nitrate concentration in groundwater [4] [6].

Consequently, the major challenge is to develop an effective and low-cost technique for a removal or reduction of nitrate concentrations in groundwater in order to preserve water quality [7]-[10]. In this context, various treatment methods have been investigated including coagulation/flocculation [11], membrane processes [12]-[16], chemical reduction [17] [18] and biological treatments [19]. Among these, electrochemical methods have emerged as one of the most promising approaches, offering ecological, technological, and economic advantages [20]-[23]. This method are gaining popularity due to transform nitrates into less harmful compounds such as nitrogen gas or ammonium [24].

Recently, our research group reported on the electrochemical denitrification using Ti/RuO<sub>2</sub> + IrO<sub>2</sub> electrodes [25]. The authors highlighted the importance of optimizing parameters such as time, current intensity, initial concentration, and pH. Therefore, the primary objective of the present study is to investigate the process through modeling based on Design of Experiments Methodology. This approach enables the evaluation of the individual effects of each factor as well as their potential interactions.

## 2. Materials and Methods

### 2.1. Chemicals and Apparatuses

All electrochemical manipulations were performed using Ti/RuO<sub>2</sub> + IrO<sub>2</sub> electrode. Electrolyses were carried out in a standard two-electrode cell, with a Voltalab 40 potentiostat, connected to an interfaced computer that employed Voltmaster 4 software. A stock solution, with a concentration of 2 g/L, was prepared by dissolving NaNO<sub>3</sub> solid (>99%, Sigma-Aldrich) in distilled water. The working solutions were subsequently obtained by successive dilutions to the desired concentrations. Nitrate concentrations (NO<sub>3</sub><sup>-</sup>) before and after electrolysis were determined by UV-visible absorption spectroscopy using a Varian UV-vis spectrophotometer Cary-60. The pH of the solutions was adjusted before electrolysis by adding NaOH or HCl solutions and measured using a HI 2211 Ph/ORP Meter pH-meter. Nitrate ion concentrations were determined according to the NFT 90-012 standard method [26]. Sodium salicylate (>99.5%, Sigma-Aldrich), Sodium azide (>99.5%, Sigma-Aldrich) and EDTA disodium salt (Sigma-Aldrich) were used as received.

## 2.2. Methods

First, an UV-Vis calibration curve was established and subsequently used to determine the nitrate concentration in all solutions before and after electrolysis. For this purpose, four sodium nitrate solutions were prepared at concentrations of 0.5, 1.0, 2.5, and 5.0 mg/L. If the concentration is outside this range, the sample is diluted. Nitrate removal efficiency was obtained by Equation (1) [27]:

$$R = \frac{(C_i - C_f)}{C_i} \times 100 \quad (1)$$

where  $C_i$  and  $C_f$  are the initial and final concentration (mg-N/L) of  $\text{NO}_3^-$ .

**Table 1** summarizes the experimental factors to be optimized and modeled using response surface methodology with Design-Expert software (version 13). The response surface methodology was used to evaluate the effects of the independent variables on the response. The experimental factors considered were electrolysis time (A), initial concentration (B), electrolysis current (C), and pH (D), while the response variable was the nitrate removal efficiency. **Table 1** presents the coded levels assigned to each factor.

**Table 1.** Process factors and their levels.

Factors	Unit	Coded variables	Levels	
			Min	Max
Electrolysis time	min	A	10	120
$\text{NO}_3^-$ concentration	mg-N/L	B	100	700
Reduction current	mA	C	-700	-100
pH		D	2	12

The matrix consisting of 4 factors, namely electrolysis time,  $\text{NO}_3^-$  concentration, reduction current and pH, is used to draw up a plan of experiments comprising 30 tests including 6 in the center.

The number of experiments  $N$  to be performed is given by the following relationship [28]:

$$N = 2k(k-1) + r \quad (2)$$

where  $r$  is the number of replicates in the centre and  $k$  is the number of factors. Thus, the mathematical equation below allowed the calculation of the response according to the factors:

$$Y = b_0 + \sum_{i=1}^n b_i x_i + \sum_{i=1}^n b_{ii} (x_i)^2 + \sum_{i=1}^{n-1} \sum_{j=i+1}^n b_{ij} x_i x_j \quad (3)$$

In this model,  $Y$  represents the predicted response (degree of conversion);  $b_0$  is the constant term;  $b_i$  are the linear coefficients;  $b_{ij}$  are the interaction coefficients; and  $b_{ii}$  are the quadratic coefficients, while  $x_i$  and  $x_j$  denote the coded values of the operating parameters.

The analysis of the different models tested (linear, two-factor interaction (2FI), quadratic, and cubic) indicates that the quadratic model is the most suitable for predicting the response. This is supported by its high statistical significance ( $p$ -value = 0.0001 < 0.05) and strong correlation coefficient ( $R^2 = 0.9551$ ), along with a satisfactory predicted  $R^2$  value of 0.8664.

Therefore, the quadratic model was selected by Design-Expert 13 to describe the relationship between the studied parameters and the response.

### 3. Results and Discussion

#### 3.1. Diagnostic Model

The comparison between the predicted values ( $Y_{\text{pred}}$ ) and the experimental values ( $Y_{\text{exp}}$ ) is presented in **Figure 1**. The results indicate a good agreement between the model predictions and the experimental response.

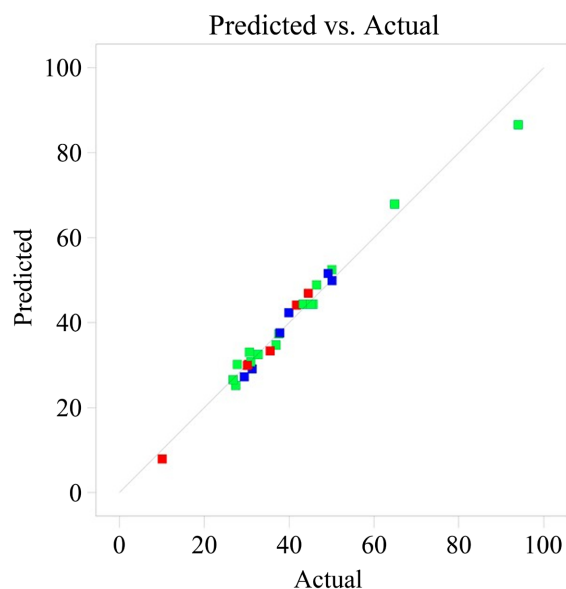


**Figure 1.** Experimental and predicted nitrate removal responses.

#### 3.2. Analyse of Variance

Analysis of variance (ANOVA) was performed using Design-Expert software [29] [30]. The Desirability Function Approach (DFA) was applied to determine the optimal operating conditions for nitrate electroreduction within the selected experimental domain. ANOVA was used to assess the significance of the model and the curvature of the response at a 95% confidence level. The significance of the process variables was evaluated based on the F-value and P-value [31] [32] with differences considered statistically significant when the P-value was less than 0.05. The nitrate removal efficiency was evaluated according to the experimental design matrix, and the corresponding results are presented in **Table 2**.

As indicated in **Table 2**, the quadratic model for nitrate removal efficiency were statistically significant ( $p \leq 0.0001$ ) [33] [34]. The results showed that only the

interaction term of BD was not significant for nitrate removal efficiency. After the removal of this term, the modified quadratic model for nitrate removal efficiency was obtained as presented in Equation (4):

$$\begin{aligned} \text{Nitrate removal efficiency} = & 59.09430 - 0.607922A - 0.133785B \\ & - 0.129728C + 3.02922D + 0.001432AB \\ & + 0.000210AC - 0.022100AD + 0.000042BC \quad (4) \\ & - 0.004548CD + 0.001783A^2 + 0.000043B^2 \\ & - 0.000139C^2 - 0.296623D^2 \end{aligned}$$

In this final fitted quadratic equation,  $A$ ,  $B$ ,  $C$  and  $D$  represent the time, the  $\text{NO}_3^-$  concentration; the reduction current; and the pH, respectively;  $AB$ ,  $AC$ ,  $AD$ ,  $BC$  and  $CD$  are the interaction terms; and  $A^2$ ,  $B^2$ ,  $C^2$ , and  $D^2$  are the square terms.

**Table 2.** Analysis of variance (ANOVA) for the quadratic response surface model.

Source	Squares	DF	Mean Square	F-value	p-value	Remarks
Model	5877.73	14	419.84	44	<0.0001	Significant
A	63.19	1	63.19	6.62	0.0212	
B	595.67	1	595.67	62.43	<0.0001	
C	417.13	1	417.13	43.71	<0.0001	
D	171.16	1	171.16	17.94	0.0007	
AB	2234.16	1	2234.16	234.14	<0.0001	
AC	47.89	1	47.89	5.02	0.0406	
AD	147.74	1	147.74	15.48	0.0013	
BC	58.22	1	58.22	6.1	0.026	
BD	0.0121	1	0.0121	0.0013	0.9721	
CD	186.19	1	186.19	19.51	0.0005	
A <sup>2</sup>	199.58	1	199.58	20.92	0.0004	
B <sup>2</sup>	102.76	1	102.76	10.77	0.005	
C <sup>2</sup>	1075.6	1	1075.6	112.72	<0.0001	
D <sup>2</sup>	377.08	1	377.08	39.52	<0.0001	
Residual	143.13	15	9.54			
Lack of Fit	138.64	10	13.86	15.44	0.0037	
Pure Error	4.49	5	0.8978			
Cor Total	6020.86	29				

DF: Degree of freedom.

### 3.3. Optimization of Physico-Chemical Parameters

The experimental results obtained at room temperature (27°C) are presented in **Table 3**. This design is based on the Box-Behnken response surface methodology.

The optimization results indicate that the most favorable conditions for nitrate removal are achieved through a specific combination of the four studied factors.

**Table 3.** Nitrate removal efficiency of electrolysis as a function of four parameters.

Time (min)	Ci (mg-N/L)	Current (mA)	pH	R (%)
65	100	-700	7	50.07
65	700	-700	7	30.96
65	100	-100	7	30.65
65	700	-100	7	26.8
10	400	-400	2	39.94
10	400	-400	12	44.54
120	400	-400	2	50.12
120	400	-400	12	30.41
10	100	-400	7	94
10	700	-400	7	27.42
120	100	-400	7	36.92
120	700	-400	7	64.8738
65	400	-700	2	29.45
65	400	-100	2	31.3
65	400	-700	12	35.54
65	400	-100	12	10.1
65	100	-400	2	49.19
65	700	-400	2	37.82
65	100	-400	12	41.75
65	700	-400	12	30.16
10	400	-700	7	46.49
10	400	-100	7	27.78
120	400	-700	7	37.59
120	400	-100	7	32.72
65	400	-400	7	43.5
65	400	-400	7	44.65
65	400	-400	7	45.21
65	400	-400	7	44.8
65	400	-400	7	43.9
65	400	-400	7	44.68

### 3.3.1. Influence of Current Intensity and pH

**Figure 2** represents the evolution of the nitrate removal efficiency as a function of the cathodic current intensity between  $-100$  and  $-700$  mA and the pH varying

from 2 to 12. These results reveal a significant interaction between these two parameters, indicating that the effect of current intensity on nitrate removal strongly depends on the pH of the solution.

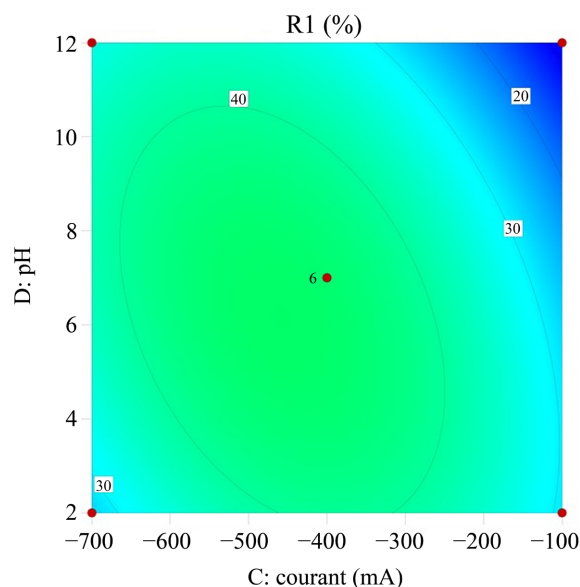


**Figure 2.** Effect of pH and cathodic current on the nitrate removal efficiency.

The analysis of the response surface reveals an elliptical region where nitrate removal efficiency reaches approximately 40% when the cathodic current ranges between  $-500$  and  $-600$  mA and the pH is between 6 and 8. However, under highly acidic conditions, increasing the absolute value of the current results in a decrease in nitrate removal efficiency, not exceeding 30%. A similar limitation is observed at low currents around  $-100$  mA. In highly basic media, the nitrate removal efficiency is also limited to about 30%, particularly at low cathodic currents (around  $-200$  mA). Within the optimal pH range of 6 to 8, increasing the cathodic current from  $-100$  to  $-700$  mA leads to a significant improvement in nitrate removal efficiency. However, at extreme pH values below 3 or above 10, the same increase in current leads in only a low nitrate removal efficiency, indicating an antagonistic interaction between extreme pH conditions and high cathodic currents. This result appears to indicate that  $H^+$  and  $OH^-$  ions compete with nitrates and affect the nitrate removal efficiency.  $H^+$  ions are reduced at approximately 0.00 V, and a high concentration of  $OH^-$  ions may hinder the mobility of nitrate ions, limiting their migration toward the cathode.

### 3.3.2. Influence of Time and pH

**Figure 3** shows the evolution of the nitrate removal efficiency as a function of the electrolysis time between 10 and 120 min.

Contrary to the effect observed for the couple (I, pH), the evolution of the nitrate removal efficiency as a function of the couple (time, pH) indicates a planar representation, with efficiency variations of up to 50%. This uniformity suggests

that the effects of pH and time are largely independent. As illustrated in **Figure 3**, the reaction exhibits high efficiency in a minimal time at pH values between 6 and 8. This result suggests good mobility of nitrate ions in a neutral medium. In acidic conditions, the nitrate removal efficiency is limited to 40%. Beyond this maximum value, any increase in electrolysis time becomes unfavorable to the process. In agreement with our previous work, this result indicates a competition between proton reduction and the desired reaction.

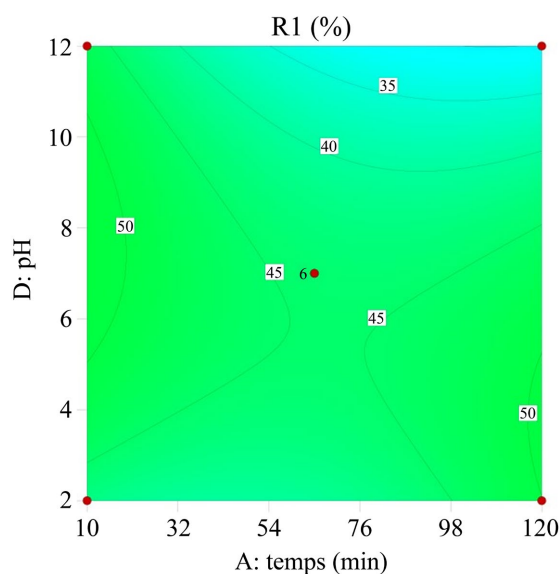


**Figure 3.** Effect of time and pH on the nitrate removal efficiency.

### 3.3.3. Influence of Time and Concentration

The following figure presents the evolution of the nitrate removal efficiency as a function of nitrate concentration.

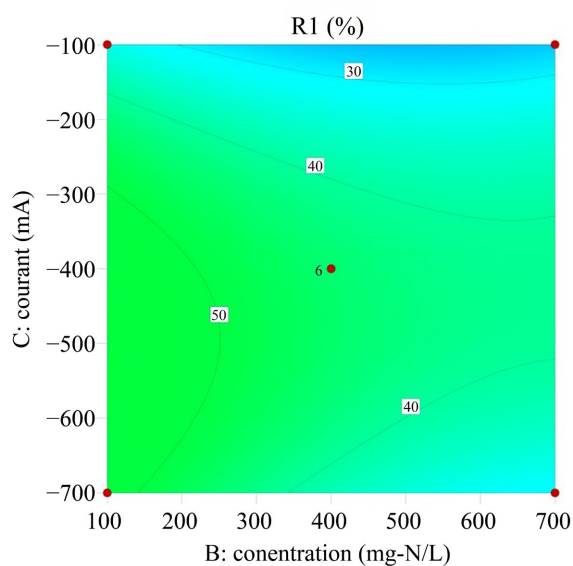


**Figure 4.** Effect of time and concentration on the nitrate removal efficiency.

**Figure 4** illustrates the combined effect of electrolysis time and nitrate concentration on the nitrate removal efficiency. At elevated  $\text{NO}_3^-$  concentrations, a decrease in removal efficiency is observed. This may be due to the inefficiency of the process above a maximum concentration value. Although, an increase in efficiency is observed at low concentration, a decrease in removal efficiency is observed with increasing electrolysis time, suggesting that excessively long treatment under these conditions may reduce nitrate removal efficiency.

### 3.3.4. Influence of Current and Concentration

**Figure 5** illustrates the evolution of the current varying between  $-100$  to  $-700$  mA in the concentration range  $100 - 700$  mg-N/L.

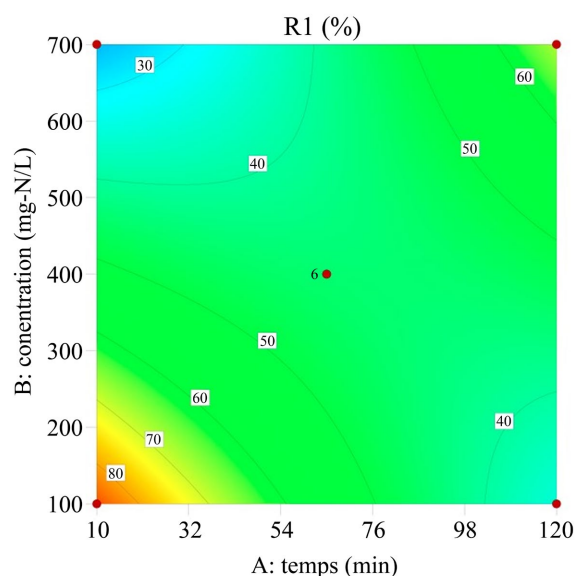


**Figure 5.** Effect of current and concentration on the nitrate removal efficiency.

The graph shows that the surface exhibits a relatively uniform undulation and gradual progression as a function of concentration and current intensity, which facilitates the identification of optimal operating conditions. As for the current intensity, it is modulated between different values in order to evaluate a wide range of reduction current. Although, the increase in the absolute value of the electric current allows a higher electron production. This behavior can be attributed to the use of two  $\text{Ti}/\text{RuO}_2 + \text{IrO}_2$  electrodes in a single-compartment cell, facilitating nitrate reduction. However, as illustrated in **Figure 5**, at high concentrations, the removal efficiency remains low even at high applied potentials and with a reduced electrode gap, indicating that other limiting factors may govern the process under these conditions.

### 3.3.5. Optimal Model Results

The optimization indicates that the initial nitrate concentration should be maintained very close to its minimum value, around  $100$  mg-N/L, which leads more efficient pollutant reduction. The optimal current intensity is strongly negative,

reflecting an intense electro-reductive regime, essential for activating the effective reduction of nitrates on the Ti/RuO<sub>2</sub> + IrO<sub>2</sub> electrode. The optimal pH, around 9.46, confirms the essential role of slightly alkaline conditions, which limit the formation of undesirable by-products such as nitrites. Furthermore, the optimal electrolysis time of 10 min shows that high nitrate removal efficiency can be achieved within a relatively short period, thereby limiting energy consumption and improving process sustainability.

### 3.3.6. Model Validation

To validate the developed model, four additional experiments were conducted under the previously determined optimal conditions: a NaNO<sub>3</sub> concentration of 100 mg-N/L, an electrolysis time of 10 minutes, and a reduction current intensity of -603 mA at a pH around 9.4. The experimental results at optimum conditions are shown in **Table 4**. The result shows good agreement between the average experimental values and the predicted values obtained from models. This result highlights a valid and applicable model for predicting the response.

**Table 4.** Verification of experimental results at optimum conditions.

Optimum conditions	Nitrate removal efficiency (%)
Mean experimental value	91.34
predicted value	91
gap	0.34

## 4. Conclusion

The objective of this study was to optimize nitrate removal by electrochemical process using the Design of Experiments methodology. Statistical analyses, particularly ANOVA, confirmed the relevance of the quadratic model, which exhibited a high coefficient of determination, indicating strong agreement between the experimental values and those predicted by the model. The results showed that current intensity and pH are the most influential parameters in the electrochemical process, while electrolysis time and concentration also affect overall treatment efficiency. The optimal operating conditions identified in this study were a reduction current intensity of -603 mA, a NaNO<sub>3</sub> concentration of 100 mg-N/L, and an electrolysis time of 10 min at a slightly basic pH. Method validation tests under these conditions showed a nitrate removal efficiency of 91%, confirming the validity of the approach. The results of this work open several promising perspectives for further development and improvement of the nitrate removal process by electro-reduction. Future studies could focus on the detailed analysis of intermediate products, such as nitrites and ammonium, to enhance the selectivity and sustainability of the process.

## Conflicts of Interest

The authors declare that there are no conflicts of interest.

## References

- [1] Wang, Q. and Yang, Z. (2016) Industrial Water Pollution, Water Environment Treatment, and Health Risks in China. *Environmental Pollution*, **218**, 358-365. <https://doi.org/10.1016/j.envpol.2016.07.011>
- [2] Srivastav, A.L., Patel, N., Rani, L., Kumar, P., Dutt, I., Maddodi, B.S., et al. (2023) Sustainable Options for Fertilizer Management in Agriculture to Prevent Water Contamination: A Review. *Environment, Development and Sustainability*, **26**, 8303-8327. <https://doi.org/10.1007/s10668-023-03117-z>
- [3] Bijay-Singh, and Craswell, E. (2021) Fertilizers and Nitrate Pollution of Surface and Ground Water: An Increasingly Pervasive Global Problem. *SN Applied Sciences*, **3**, Article No. 518. <https://doi.org/10.1007/s42452-021-04521-8>
- [4] Dimé, A.K.D., Diouf, G., Dramé, E.T. and Fall, M. (2018) Caractérisation Physico-Chimique de la Nappe Phréatique Située dans une Zone à Forte Pollution Industrielle: Cas de la Commune de Ngoundiane. *Journal de la Société Ouest-Africaine de Chimie*, **46**, 23-28.
- [5] Katabami, K., Hayakawa, M. and Gando, S. (2016) Severe Methemoglobinemia due to Sodium Nitrite Poisoning. *Case Reports in Emergency Medicine*, **2016**, Article ID: 9013816. <https://doi.org/10.1155/2016/9013816>
- [6] Dimé, A.K.D., Diouf, G., Sarr, M.M. and Fall, M. (2020) Caractérisation Physico-Chimique de la Nappe Phréatique Située dans une Zone à Forte Pollution Industrielle: Cas de la Commune de Rufisque. *Revue Ivoirienne des Sciences et Technologie*, **35**, 163-174.
- [7] Kou, X., Ding, J., Li, Y., Li, Q., Mao, L., Xu, C., et al. (2021) Tracing Nitrate Sources in the Groundwater of an Intensive Agricultural Region. *Agricultural Water Management*, **250**, Article ID: 106826. <https://doi.org/10.1016/j.agwat.2021.106826>
- [8] Diouf, G., Dime, A.K.D., Dia, A., Yatt, B. and Fall, M. (2024) Caractérisation physico-chimique des sols situés dans une zone à forte pollution industrielle: Cas des communes de Ngoundiane et de Rufisque au Sénégal. *International Journal of Biological and Chemical Sciences*, **18**, 1128-1139. <https://doi.org/10.4314/ijbcs.v18i3.32>
- [9] Riaz, M., Ahmad, M.N., Mukhtar, M., Aqsa, and Nawaz, N. (2024) Nitrate Contamination of Soil and Water: Implications for Ecosystem Functions and Human Health. In: Naidu, R., Ed., *Inorganic Contaminants and Radionuclides*, Elsevier, 351-373. <https://doi.org/10.1016/b978-0-323-90400-1.00001-x>
- [10] Diouf, G., Dime, A.K.D., Boye, M.B., Balde, I., Kane, C. and Fall, M. (2022) Optimisation des Paramètres Influençant le Rendement de la Dénitrification Electrochimique de l'Eau par l'Electrode de Ti/RuO<sub>2</sub> + IrO<sub>2</sub>. *Afrique Science*, **20**, 1-10.
- [11] Zaki, N., Charki, A., Hadoudi, N., Fraiha, O., El Ouarghi, H., Salhi, A., et al. (2024) Coagulation-Flocculation Parameters for Simultaneous Removal of Nitrates, Nitrites, Phosphates, and Ammonium from Wastewater: A Mini Review. *E3S Web of Conferences*, **527**, Article ID: 03015. <https://doi.org/10.1051/e3sconf/202452703015>
- [12] Boppella, R., Ahmadi, M., Arndt, B.M., Lustig, D.R. and Nazemi, M. (2024) Pulsed Electrolysis in Membrane Electrode Assembly Architecture for Enhanced Electrochemical Nitrate Reduction Reaction to Ammonia. *ACS Catalysis*, **14**, 18223-18236. <https://doi.org/10.1021/acscatal.4c05225>
- [13] Wang, X., Wu, X., Ma, W., Zhou, X., Zhang, S., Huang, D., et al. (2023) Free-standing Membrane Incorporating Single-Atom Catalysts for Ultrafast Electroreduction of Low-Concentration Nitrate. *Proceedings of the National Academy of Sciences of the*

- United States of America*, **120**, e2217703120.  
<https://doi.org/10.1073/pnas.2217703120>
- [14] Ma, J., Wei, W., Qin, G., Xiao, T., Tang, W., Zhao, S., *et al.* (2022) Electrochemical Reduction of Nitrate in a Catalytic Carbon Membrane Nano-Reactor. *Water Research*, **208**, Article ID: 117862. <https://doi.org/10.1016/j.watres.2021.117862>
- [15] Fan, Y., Wang, X., Butler, C., Kankam, A., Belgada, A., Simon, J., *et al.* (2024) Highly Efficient Metal-Free Nitrate Reduction Enabled by Electrified Membrane Filtration. *Nature Water*, **2**, 684-696. <https://doi.org/10.1038/s44221-024-00278-7>
- [16] Pirrone, N., Garcia-Ballesteros, S., Hernández, S. and Bella, F. (2024) Membrane/electrolyte Interplay on Ammonia Motion Inside a Flow-Cell for Electrochemical Nitrogen and Nitrate Reduction. *Electrochimica Acta*, **493**, Article ID: 144415. <https://doi.org/10.1016/j.electacta.2024.144415>
- [17] Liou, Y., Lo, S., Lin, C., Kuan, W. and Weng, S. (2005) Chemical Reduction of an Unbuffered Nitrate Solution Using Catalyzed and Uncatalyzed Nanoscale Iron Particles. *Journal of Hazardous Materials*, **127**, 102-110. <https://doi.org/10.1016/j.jhazmat.2005.06.029>
- [18] Rodríguez-Maroto, J.M., García-Herruzo, F., García-Rubio, A., Gómez-Lahoz, C. and Vereda-Alonso, C. (2009) Kinetics of the Chemical Reduction of Nitrate by Zero-Valent Iron. *Chemosphere*, **74**, 804-809. <https://doi.org/10.1016/j.chemosphere.2008.10.020>
- [19] Rezvani, F., Sarrafzadeh, M., Ebrahimi, S. and Oh, H. (2017) Nitrate Removal from Drinking Water with a Focus on Biological Methods: A Review. *Environmental Science and Pollution Research*, **26**, 1124-1141. <https://doi.org/10.1007/s11356-017-9185-0>
- [20] de Santana, M.M., Zanoelo, E.F., Benincá, C. and Freire, F.B. (2018) Electrochemical Treatment of Wastewater from a Bakery Industry: Experimental and Modeling Study. *Process Safety and Environmental Protection*, **116**, 685-692. <https://doi.org/10.1016/j.psep.2018.04.001>
- [21] Baldé, I., Dimé, A.K.D. and Kane, C. (2023) Production Electrochimique de la Soude: Optimisation et Modélisation du Procédé par la Méthodologie de Surface de Réponse. *Afrique Science*, **22**, 29-41.
- [22] Duan, W., Li, G., Lei, Z., Zhu, T., Xue, Y., Wei, C., *et al.* (2019) Highly Active and Durable Carbon Electrocatalyst for Nitrate Reduction Reaction. *Water Research*, **161**, 126-135. <https://doi.org/10.1016/j.watres.2019.05.104>
- [23] Teng, M., Ye, J., Wan, C., He, G. and Chen, H. (2022) Research Progress on Cu-Based Catalysts for Electrochemical Nitrate Reduction Reaction to Ammonia. *Industrial & Engineering Chemistry Research*, **61**, 14731-14746. <https://doi.org/10.1021/acs.iecr.2c02495>
- [24] Babrauskas, V. and Leggett, D. (2019) Thermal Decomposition of Ammonium Nitrate. *Fire and Materials*, **44**, 250-268. <https://doi.org/10.1002/fam.2797>
- [25] Boye, M.B., Dimé, A.K.D., Diop, A., Kane, C. and Fall, M. (2023) Process Optimization and Modeling by Response Surface Methodology of Nitrite Electro-Reduction by Ti/RuO<sub>2</sub> + IrO<sub>2</sub> Electrode. *American Journal of Analytical Chemistry*, **14**, 531-540. <https://doi.org/10.4236/ajac.2023.1412031>
- [26] Sghiouer, F.E., Nahli, A., Bouka, H. and Chlaida, M. (2024) Analysis of the Drought Effects on the Physicochemical and Bacteriological Quality of the Inaouene River Water (Taza, Morocco). *Scientific African*, **25**, e02328. <https://doi.org/10.1016/j.sciaf.2024.e02328>
- [27] Emamjomeh, M.M., Jamali, H.A. and Moradnia, M. (2017) Optimization of Nitrate

- Removal Efficiency and Energy Consumption Using a Batch Monopolar Electrocoagulation: Prediction by RSM Method. *Journal of Environmental Engineering*, **143**, Article ID: 04017022. [https://doi.org/10.1061/\(asce\)ee.1943-7870.0001210](https://doi.org/10.1061/(asce)ee.1943-7870.0001210)
- [28] Auta, M. (2012) Optimization of Tea Waste Activated Carbon Preparation Parameters for Removal of Cibacron Yellow Dye from Textile Waste Waters. *International Journal of Advanced Engineering Research and Studies*, **1**, 50-56.
- [29] Hassan, A., Samy, G., Hegazy, M., Balah, A. and Fathy, S. (2024) Statistical Analysis for Water Quality Data Using ANOVA (Case Study—Lake Burullus Influent Drains). *Ain Shams Engineering Journal*, **15**, Article ID: 102652. <https://doi.org/10.1016/j.asej.2024.102652>
- [30] Litu, L., Buema, G., Mosoarca, G. and Harja, M. (2024) Copper Ion Removal by Adsorption Using Fly Ash-Based Geopolymers: Process Optimization Insights from Taguchi and ANOVA Statistical Methods. *Materials*, **17**, Article 3992. <https://doi.org/10.3390/ma17163992>
- [31] Gebresemati, M., Gabbiye, N. and Sahu, O. (2017) Sorption of Cyanide from Aqueous Medium by Coffee Husk: Response Surface Methodology. *Journal of Applied Research and Technology*, **15**, 27-35. <https://doi.org/10.1016/j.jart.2016.11.002>
- [32] Elmoubarki, R., Taoufik, M., Moufti, A., Tounsadi, H., Mahjoubi, F.Z., Bouabi, Y., Qourzal, S., Abdennouri, M. and Barka, N. (2017) Box-Behnken Experimental Design for the Optimization of Methylene Blue Adsorption onto Aleppo Pine Cones. *Journal of Materials and Environmental Sciences*, **8**, 2184-2191.
- [33] Albavera-Mata, A., Gázquez, J.L. and Vela, A. (2025) Generalized Quadratic Model for Charge Transfer. *Physical Chemistry Chemical Physics*, **27**, 11318-11330. <https://doi.org/10.1039/d5cp00866b>
- [34] Beyene, K.A. (2022) Comparative Study of Linear and Quadratic Model Equations for Prediction and Evaluation of Surface Roughness of a Plain-Woven Fabric. *Research Journal of Textile and Apparel*, **27**, 281-298. <https://doi.org/10.1108/rjta-08-2021-0107>